Iron encrustations on filamentous algae colonized by *Gallionella*-related bacteria in a metal-polluted freshwater stream

J. F. Mori[1], T. R. Neu[2], Shipeng Lu[1,3], M. Händel[4], K. U. Totsche[4], and K. Küsel[1,3]

[1] Institute of Ecology, Aquatic Geomicrobiology, Friedrich Schiller University Jena, Dornburger Strasse 159, 07743 Jena, Germany

[2] Department of River Ecology, Helmholtz Centre for Environmental Research – UFZ, Brueckstrasse 3A, 39114 Magdeburg, Germany

[3] German Centre for Integrative Biodiversity Research (iDiv) Halle-Jena-Leipzig, Deutscher Platz 5e, 04103 Leipzig, Germany

[4] Institute of Geosciences, Hydrogeology, Friedrich Schiller University Jena, Burgweg 11, 07749 Jena, Germany

Correspondence to: Kirsten Küsel (Kirsten.Kuesel@uni-jena.de)

Abstract

Filamentous macroscopic algae were observed in slightly acidic to circumneutral (pH 5.9~6.5) metal-rich stream water that leaked out from a former uranium-mining district (Ronneburg, Germany). These algae differ in color and morphology and were encrusted with Fe-deposits. To elucidate the potential interaction with Fe(II)-oxidizing bacteria (FeOB), we collected algal samples at three time points during summer 2013 and studied the algae-bacteria-mineral compositions via confocal laser scanning microscopy (CLSM), scanning electron microscopy, Fourier transform infrared spectra, and a 16S and 18S rRNA gene based bacterial and algae community analysis. Surprisingly, sequencing analysis of 18S rRNA gene regions of green and brown algae revealed high homologies with the freshwater algae *Tribonema* (99.9~100%). CLSM imaging indicates a loss of active chloroplasts in the algae cells, which may be responsible for the change in color in *Tribonema*. Fe(III)-precipitates on algal cells identified as ferrihydrite and schwertmannite were associated with microbes and extracellular polymeric substances (EPS)-like glycoconjugates. While the green algae were fully encrusted with Fe-precipitates, the brown algae often exhibited discontinuous series of precipitates. This pattern was likely due to the intercalary growth of algal filaments which allowed them to avoid detrimental encrustation. 16S rRNA gene targeted studies based on DNA and RNA revealed that *Gallionella*-related FeOB dominated the bacterial RNA and DNA communities (70-97% and 63-96%, respectively) suggesting their capacity to compete with the abiotic Fe-oxidation under the fully oxygen-saturated conditions that occur in association with photosynthetic algae. Quantitative PCR revealed even higher *Gallionella*-related 16S rRNA gene copy numbers on the surface of green algae compared to the brown algae. The latter harbored a higher microbial diversity, including some putative predators of algae. Lower photosynthetic activities of the

Deleted: in

Deleted: ic

Deleted: yellow-green

Deleted: fatal

Deleted: contribution to Fe(II) oxidation

brown algae could have led to reduced EPS production which is known to affect predator colonization. Collectively, our results suggest that metal-tolerant *Tribonema* sp. provide suitable microenvironments even for neutrophilic FeOB which goes against current dogma of these bacteria being strict microaerophiles.

Deleted: lead

Deleted: may have enabled

Deleted: The differences observed between green and brown algae

Deleted: microaerophilic Fe-oxidizing bacteria. However, high levels of iron orchres can be fatal to the alga.

1. Introduction

Algae are known to inhabit all freshwater ecosystems including rivers, streams, lakes and even small water volumes present in pitcher plants (Stevenson et al., 1996; Cantonati and Lowe, 2014; Gebühr et al., 2006). Macroscopic algae often bloom rapidly in rivers and in small freshwater streams, such as groundwater effluents (Stevenson et al., 1996), through germination of spores, vegetative growth and reproduction (Transeau, 1916). As primary producers, these algae provide benefits for other organisms by supplying them with organic matter and oxygen via photosynthesis and are often surrounded by associated microbes (Haack and McFeters, 1982; Geesey et al., 1978; Cole, 1982; Azam, 1998). Unicellular and multicellular algae can produce polysaccharides like extracellular polymeric substances (EPS) as a shunt for carbon produced in excess during photosynthesis (Wotton, 2004; Liu and Buskey, 2000). Due to these functions, algae likely affect the activities of co-existing microbes and play important roles in microbial ecology in streams.

Deleted: , especially during cell senescence

Some algal species have been detected in metal-polluted streams, such as hot spring effluents (Wiegert and Mitchell, 1973) and mining-impacted sites (Reed and Gadd, 1989; Warner, 1971). These algae are known to be tolerant or resistant to high concentration of metals such as Zn, Cu, Cd, Pb, Fe, and As (Reed and Gadd, 1989; Foster, 1977, 1982) and some are capable of accumulating metals (Fisher et al., 1998; Yu et al., 1999; Greene et al., 1987) which makes them ideal candidates for bio-remediation of metal-polluted sites (Yu et al., 1999; Malik, 2004). Green algae, such as *Ulothrix*, *Microspora*, *Klebsormidium*, and *Tribonema*, occur in acid mine drainage (AMD)-impacted sites (Warner, 1971; Winterbourn et al., 2000; Das et al., 2009), sometimes forming heterogeneous streamer communities (Rowe et al., 2007). Although some of

these algae show iron ochre depositions, their interactions with Fe(II)-oxidizing bacteria are not well characterized.

A group of prokaryotes called Fe(II)-oxidizing bacteria (FeOB) mediates the oxidation of Fe(II) to Fe(III) to conserve energy for growth (Colmer and Hinkle, 1947; Hanert, 2006). Most FeOB are autotrophs (Johnson and Hallberg, 2009; Kappler and Straub, 2005). Biogenic Fe(III) subsequently hydrolyzes and precipitates from solution forming various Fe(III)-oxides when the pH exceeds 2 (Johnson et al., 2014). Aerobic acidophilic Fe(II)-oxidizers are the main drivers of Fe(II)-oxidation in acidic and iron-rich freshwater environments due to low rates of chemical Fe(II)-oxidation under acidic conditions (Leduc and Ferroni, 1994; Hallberg et al., 2006; Tyson et al., 2004; López-Archilla et al., 2001; Senko et al., 2008; Kozubal et al., 2012). In contrast, neutrophilic FeOB, such as *Gallionella* spp., *Sideroxydans* spp., or *Leptothrix* spp., have to compete with a rapid chemical Fe(II)-oxidation at circumneutral pH and thus often inhabit oxic-anoxic transition zones, such as sediment-water surfaces (Emerson and Moyer, 1997; Peine et al., 2000; Hedrich et al., 2011b) or the rhizosphere of wetland plants, where the plant roots leak oxygen and FeOB deposit Fe-minerals (known as 'Fe-plaques') on plant root surfaces (Neubauer et al., 2002; Johnsongreen and Crowder, 1991; Emerson et al., 1999). *Gallionella* spp. are chemolithoautotrophs that prefer microoxic conditions (Emerson and Weiss, 2004; Lüdecke et al., 2010).

We observed macroscopic streamer-forming algae in slightly acidic to circumneutral (pH 5.9~6.5), metal-rich stream water flowing out of passively flooded abandoned underground mine shafts in the former Ronneburg uranium mining district in Germany. This seeping groundwater creates new streams and iron-rich terraces at an adjacent drainage creek bank. The filamentous algae present during the summer months differed mainly in color, but all types showed iron

Deleted: 1981

Deleted: for

Deleted: ,

Deleted: with 13-20% oxygen saturation

Deleted: Acidophilic and neutrophilic FeOB can produce EPS, which can be used to protect the cells against encrustation with Fe(III)-minerals by acting as a barrier to prevent accumulation of Fe(III)-minerals directly on cell surfaces. This defense mechanism is especially important for FeOB growing above pH 2. EPS can also accelerate bacterial Fe(II)-oxidation by catching free Fe(II) in the water and localizing microbially formed Fe-oxides in proximity to the cells, which allow bacteria to utilize the proton gradient for energy generation (Chan et al., 2004). EPS-producing acidophilic FeOB, such as *Acidithiobacilllus* spp., *Ferrovum* spp., *Leptospirillum* spp., and *Acidimicrobium* spp., are known for their gelatinous, filamentous macroscopic growth in flowing waters (Wakao et al., 1985; Bond et al., 2000; Hallberg et al., 2006; Kay et al., 2013). Recently, a pure culture of *Ferrovum myxofaciens* was shown to produce copious amounts of EPS, composed mainly of polysaccharides and proteins, which allows the cells to attach to each other and solid surfaces, preventing the cells from being washed out in flowing systems (Johnson et al., 2014b). This streamer-like growth appears to be particularly important in extreme environments. ¶

ochre deposits. Since high abundances of *Gallionella*-related FeOB were detected in the seeping water and the drainage creek in previous studies (Fabisch et al., 2013, 2015), potential interactions between these neutrophilic FeOB and the streamer-forming algae communities were suggested.

Few studies have addressed the relationship between Fe(II)-oxidation and algae. A previous study reported that oxygen production by cyanobacteria appeared to control Fe(II)-oxidation in iron-rich microbial mats at Chocolate Pots in Yellowstone despite co-existence of anoxygenic photosynthetic FeOB (Trouwborst et al., 2007), but there was no evidence of biogenic Fe(II)-oxidation by chemolithotrophic neutrophilic FeOB. Another study examining a bicarbonate Fe(II)-rich spring in the Swiss Alps showed the co-existence but physical separation of cyanobacteria and *Gallionellaceae* (Hegler et al., 2012). Since the presence and activity of neutrophilic FeOB close to oxygen-generating photosynthetic organisms has not been documented, we applied different microscopic techniques to localize the Fe-minerals and microorganisms on the algal surfaces and compared the bacterial community structure of different algal samples to learn more about these multi-species interactions in metal-polluted environments.

Deleted: Thus,

2. Materials and Methods

2.1. Field site and sampling

Algal samples were taken in the outflow water in the former Ronneburg uranium-mining district (Thuringia, Germany) in 2013. This district in eastern Germany was one of the largest uranium mining operations in the world which produced 113,000 metric tons of uranium primarily through heap-leaching with sulfuric acid between 1945 and German reunification in 1990. After

the mines were closed, the open pit was filled with waste rock from the leaching heaps to prevent further acid mine drainage (AMD). The underground mines were flooded and treated with alkali to buffer the water to a more neutral pH. The mine water outflow began in 2010 when the water table rose and contaminated water from the underground mine reached the surface of surrounding grassland. The mine water outflow flowed 20 m down a hillside into the creek (Fig. 1) where red-orange terraces enriched with the Fe-oxyhydroxides goethite and ferrihydrite formed (Johnson et al., 2014; Fabisch et al., 2015).

We sampled algae of green and brown color in July, August and September from four different sites beginning at the outflow water (site O) and three sites further downstream (A, B, C) which were separated from O by some artificial impoundments; the distance between A and C was 8.8 m (Fig. 1). In July 2013, we could not reach site O because it was fenced due to construction work. Chemical parameters of water (pH, temperature, Eh, and oxygen concentration) were measured in situ at every sampling time, using respective electrodes and meters (Mettler Toledo; WTW, Switzerland). In addition, water collected from each site was filtered with 0.45 µm poly vinylidene fluoride (PVDF) and acidified with HCl or HNO_3 on site and stored at 4°C until the measurements of metals, sulfate, and organic carbon (DOC) concentrations. Algae and sediment samples were taken from the stream with a sterilized spatula and stored at 4°C for microscopic analyses or at -80°C for molecular biological experiments, respectively.

2.2. Geochemical characterization of the stream

Concentration of Fe(II) in water was detected using the phenanthroline method (Tamura et al., 1974) and total Fe was determined following the addition of ascorbic acid (0.6% final concentration). Sulfate concentration was determined using the barium chloride method (Tabatabai, 1974). DOC in water was measured by catalytic combustion oxidation using TOC

Deleted: with

Deleted: after

analyzer (TOC-V CPN, Shimadzu, Japan). Dissolved metals (Fe, Mn, Ni, and U) in stream water were measured using inductively coupled mass spectrometry (ICP-MS; X-Series II, Quadrupol, Thermo Electron, Germany). Metals which accumulated on the sediments and the algae were determined by ICP-MS and ICP-optical emission spectrometry (ICP-OES, 725ES, Varian, Germany) after digestion. The algae sample taken at site C in August 2013 and stored at 4°C was washed with deionized water on a petri dish to remove big sediment particles, then followed by drying (200°C, overnight), grinding and microwave digestion (Mars XPress, CEM, Germany) using HNO_3 for ICP-MS/OES measurements. The sediment samples taken at each sampling site were also dried and ground, and then 0.1-0.5 g of sediments were digested using 2 ml HNO_3, 3 ml HF, and 3 ml $HClO_4$ for ICP-MS/OES measurements.

2.3. Observation of algae under light microscope

The fresh algal samples were observed on the same day as sampling under light microscope (Axioplan, Zeiss, Germany). Small pieces (~5 mm) of algal bundles were picked, placed on a glass slide with small amount of stream water, and then covered with a glass coverslip. Microscopic images in bright field were taken with digital camera ProgRes CS (Jenoptik, Germany).

Deleted: just after sampling

2.4. CLSM imaging

The algal samples collected in September were examined by confocal laser scanning microscopy (CLSM) using a TCS SP5X (Leica, Germany). The upright microscope was equipped with a white laser source and controlled by the software LAS AF version 2.4.1. Samples were mounted in a 0.5 µm deep CoverWell™ (Lifetechnologies) chamber and examined with a 63× NA 1.2 water immersion lens. Algal-associated bacteria were stained with Syto9, a nucleic acid specific fluorochrome. Fluorescently labelled lectin (AAL-Alexa448, Linaris), which preferentially binds

Deleted: taken

Deleted: Syto9

to fucose linked (α-1, 6) to *N*-acetylglucosamine or to fucose linked (α-1, 3) to *N*-acetyllactosamine related structures and can be applied for detection of algal cell walls (Sengbusch and Müller, 1983) and the microbial EPS complex (Neu et al., 2001) was used to stain and detect glycoconjugates. The recording parameters were as follows: excitation at laser lines 488, 568, 633 nm; emission recorded at 483-493 (reflection), 500-550 (Syto9), 580-620 (possible autofluorescence), 650-720 (chlorophyll A). Optical sections were collected in the Z-direction with a step of 1 µm. Images were deconvolved using the option 'classic maximum likelihood estimation' from Huygens version 14.06 (SVI). Lastly, image data sets were projected by Imaris version 7.7.2 (Bitplane).

Deleted: ,

2.5. SEM-EDX

Scanning electron microscopy (SEM) was used to study the morphology of mineral precipitates on algal surfaces. Droplets of sample suspensions were placed on silicon wafers and subjected to air drying. High-resolution secondary electron (SE) images and energy dispersive X-ray spectroscopy (EDX) were taken with an ULTRA plus field emission scanning electron microscope (Zeiss).

2.6. FTIR measurement for mineral precipitates on algae

Fourier transform infrared (FTIR) spectra of algae encrusted with Fe-minerals were recorded using a Nicolet iS10 spectrometer (Thermo Fisher Scientific, Dreieich, Germany). Mortared samples were mixed with KBr (FTIR grade, Merck, Darmstadt, Germany) at a ratio of 1:100 and pressed into pellets. The pellets were studied in transmission mode in the mid-infrared range between 4000 and 400 cm^{-1} for a total of 16 scans at a resolution of 4 cm^{-1}. Spectra were baseline corrected by subtracting a straight line running between the two minima of each spectrum and normalized by dividing each point by the spectrum's maximum.

2.7. Total nucleic acids extraction from algae-microbial communities

Total nucleic acids of algae-microbial communities were extracted from ~1.4 g wet weight of algal bundle via bead beating in $NaPO_4$ buffer (pH 8.0) with TNS solution (500 mM Tris-HCl pH 8.0, 100 mM NaCl, 10% SDS wt/vol). The supernatant was taken after centrifugation, followed by extraction with equal volumes of phenol-chloroform-isoamyl alcohol [PCI, 25:24:1 (vol:vol:vol), AppliChem] and chloroform-isoamyl alcohol [CI, 24:1 (vol:vol), AppliChem]. Nucleic acids were precipitated with two volumes of polyethylene glycol (PEG) by centrifugation at 20,000 *g* and 4°C for 90 min. The pellets were washed with ice-cold 70% ethanol and suspended in 50 µl elution buffer (EB, Qiagen).

2.8. 18S rRNA gene-based identification of algal species

The 18S rRNA gene region of the DNA extracted from algae-microbial communities was amplified by PCR employing the universal primer pair Euk20F/Euk1179R (Euringer and Lueders, 2008) or the *Chlorophyta*-targeting primer pair P45/P47 (Dorigo et al., 2002). The PCR reactions using both primer pairs were as follows: initial denaturing at 94°C for 5 min, 25-30 cycles of denaturing at 94°C for 30 s, annealing at 57°C for 30 s, and extension at 72°C for 90 s, and followed by final extension at 72°C for 10 min. Amplified products were purified through a spin column (NucleoSpin Gel and PCR Clean-up, Macherey-Nagel, Germany) and sequenced using Sanger technology (Macrogen Europe, Amsterdam, The Netherlands). Sequences were processed using Geneious 4.6.1 for trimming and assembling, followed by the BLAST homology search.

2.9. Quantitative PCR

Quantitative PCR was performed to elucidate the 16S rRNA gene copy numbers of *Gallionella* colonizing the algae surface using 16S rRNA gene-targeted primers specific for *Gallionella* spp.

(Gal122F, 5'-ATA TCG GAA CAT ATC CGG AAG T -3'; Gal384R, 5'- GGT ATG GCT GGA TCA GGC -3') (Heinzel et al., 2009). Aliquots of 1.25 ng DNA were used in triplicate as the template for qPCR using the Mx3000P real-time PCR system (Agilent, USA) and Maxima SYBR Green qPCR Mastermix (Fermentas, Canada). Standard curves were prepared by serial dilution of plasmid DNA containing the cloned 16S rRNA gene sequence of *Gallionella* (accession no. JX855939). Melting curve analysis was used to confirm the specificities of the qPCR products. PCR grade water and TE buffer were included as non-template controls. Detailed qPCR conditions were described by Fabisch et al. (Fabisch et al., 2013).

2.10. Amplicon pyrosequencing

16S rRNA gene-targeted amplicon pyrosequencing was performed to reveal the population structures of bacteria on the algae. To determine the bacterial community composition based on RNA, cDNA samples were prepared as follows: 3.3-6.0 µg of total nucleic acids extracted from algae-microbial communities were treated with DNase using TURBO DNA-*free*™ Kit (Ambion, USA) to remove all DNA, and then 0.3-0.5 µg of DNase-treated RNA samples were transcribed to cDNA using RETROscript® Kit (Life Technologies, CA) and stored at -20°C. The total nucleic acid samples (as DNA samples) and cDNA samples were sent to the Research and Testing Laboratory (Lubbock, TX, USA) for pyrosequencing of the V4-V6 region. Samples were sequenced on a Roche 454 FLX system using tags, barcodes and forward primers listed in Table S1. Sequence reads were processed in Mothur 1.33.0 (Schloss et al., 2009) for trimming, quality checking, screening, chimera removal, and alignment based on the Silva reference alignment files provided on the Mothur website (http://www.mothur.org/wiki/Silva_reference_files). Dendrograms were constructed in Mothur using unweighted pair group method arithmetic averages (UPGMA) based on Bray-Curtis index (Bray and Curtis, 1957) to estimate similarity

among bacterial DNA and RNA community compositions in each sample. Sequences originating from algal chloroplasts were removed for statistical analysis of community composition. Gini-Simpson index was calculated using Mothur.

3. Results

3.1. Characterization of algae-bacterial assemblage

Abundant macroscopic filamentous algae up to 10 cm length appeared at the outflow site (O) (Fig. 1) and further downstream at sites A, B, and C during the summer months. Algae were often covered by orange-colored minerals. The outflow water was suboxic (1.3-2.0 mg l^{-1} oxygen) at site O with a slightly acidic pH of 5.9, however, water became more oxygenated (6.2-6.9 mg l^{-1} oxygen) and had a higher pH (6.4-6.5) further downstream (Fig. 2). The increase in oxygen could be caused by both turbulent mixing with air and photosynthetic activities of the algae and increase of pH likely resulted from a combination of CO_2 outgassing from the initial anoxic outflow water and draw down of CO_2 via algal growth. The water temperature was approximately 14-17°C at site O during sampling. Dissolved iron in the water was primarily in the form of Fe(II) with maximum concentrations of 3.3 mM and decreased in concentration (to 2.1 mM) as the water moved downstream towards sites A, B, and C. The other parameters measured did not indicate distinct differences between the sites O, A, B, and C (Eh, 140-180 mV; conductivity, 4.8-4.9 ms cm^{-1}; DOC, 3.0-4.5 mg l^{-1}; sulfate concentration, 30-35 mM; Fig. 2). The stream water was also enriched with other metals including Mn, Ni, Zn and U.

In July 2013, we sampled green algae from sites A and B (algae at site O could not be reached), and brown algae from site C. During a subsequent sampling during August 2013, the algae collected from site B changed in color from green to brown, while algae samples collected from

Deleted: I

Deleted: and pH

Deleted: degassing of CO_2

Deleted: W

Deleted: ; these water temperature values are likely due to the underground exothermic pyrite oxidation (Johnson et al., 2014a)

sites O and A still appeared green. By September 2013, most algae had disappeared; only small amounts of green algae were left at site O and some brown algae at site A (Table 1). Sequencing analysis of 18S rRNA gene regions amplified from DNA extracts of green and brown algae showed that all algae had high homologies with *Tribonema* spp. (*T. viride*, *T. minus*, *T. ulotrichoides*, 99.9~100%; Table S2), a genus of freshwater algae belonging to the class of *Xanthophyceae*.

Microscopic observations revealed unbranched filamentous algae with a single cell length of 30-50 µm and a cell diameter of 8-10 µm (Fig. 3C, D, 4A, B, C). Green algae cells yielded 10-15 visible chloroplasts which exhibited strong autofluorescence, whereas brown algae cells contained only 5-7 countable chloroplasts and displayed weaker autofluorescence. The brown algae often showed green autofluorescence under UV-light exposure (data not shown), which likely resulted from flavin-like molecules or luciferin compounds (Tang and Dobbs, 2007). This green autoflouresence was not detected in the green algae, likely due to stronger signals from chloroplasts. According to the cell morphology and number of chloroplasts per cell, the green and brown algae display a high degree of similarity to *T. viride* comparing to *T. minus* and *T. ulotrichoides* (Akiyama et al., 1977; Gudleifsson, 1984; H. Wang et al., 2014).

Minerals adhered to and were distributed in a regular discontinuous pattern on the surface of the brown algae. In contrast, the surface of the green algae was encrusted with minerals in irregular shape, size and location (Fig. 3C, D, 4A, B). CLSM images using Syto9 stain showed minerals adhered to the surface of both brown and green algae that were colonized by microorganisms (Fig. 4A, B). These microbial cells primarily colonized the minerals attached to the algae surfaces, while a smaller proportion of microbial cells were adhered directly to the algae bodies. Neither stalks of *Gallionella* nor other characteristic extracellular structures of FeOB were found

Deleted: species

Deleted: yellow-green

Deleted:

Deleted:

Deleted: , however

Deleted: in a random arrangement and with roughly shaped minerals

Deleted: (or thin layer of minerals on the algae)

on the algae. CLSM images with lectin staining showed the cell sections in algal filaments were distributed between regularly located Fe-minerals. In addition, algal or bacterial EPS-like glycoconjugates were likely associated with the minerals (Fig. 4C), whereas the amount of EPS could not be quantified or compared between the green and brown algae.

3.2. Component analysis of mineral precipitates on the algae

Secondary electron (SE) images with EDX analyses showed sulfur-containing Fe-oxides almost completely covered the surface of the green algae (Fig. 5A, 6A), whereas some areas on the surface of the brown algae were not encrusted (Fig. 5B, 6B). The non-encrusted parts of the brown algae primarily displayed background signal (i.e. Si signal of the sample holder). Weak signals of C, Mg, Ca and P were also detected by EDX. The elemental composition of Fe-oxides not associated with algae was almost identical to those of the encrusted algae, suggesting mineral composition was not affected by biological activity.

FTIR spectra exhibited signals of ferrihydrite and schwertmannite (Fig. 6C). Their presence was also confirmed by high resolution SE images. Spherical aggregates with nano-needles on the surface edges are defining characteristics for schwertmannite (Fig. S1), while aggregates with no single crystallites are often composed of ferrihydrite (Carlson et al., 2002). The FTIR spectra of minerals on the green algae also showed weak signals of Si-O bonding at 1030 cm^{-1}, which might be due to residual clay minerals.

Total extractions of the brown algae collected at site C revealed that in addition to Fe, Mn, Ni, Zn and U accumulated on the algae surface similarly to the underlying sediments at site C (Fig. S2); Fe and U even showed higher concentrations on the surface of the algae in comparison to the sediment (540 mg of Fe and 910 µg of U in 1 gdw algae and 390-660 mg of Fe and 90-750 µg of U in 1 gdw sediment).

Deleted: which

Deleted: .

Deleted: S

Deleted: parts

3.3. Elucidating the bacterial community structure associated with algae

Quantitative PCR detected high gene copy numbers (per gram wet weight algae) for *Gallionella*-related 16S rRNA with slightly higher numbers for the green algae ($1.72 \times 10^9 – 7.08 \times 10^9$) compared to brown algae (Table 1). Similarly, 16S rRNA gene-targeted amplicon pyrosequencing revealed that members of the *Gallionellaceae* were the dominant bacterial group within these algae-microbial communities when comparing both DNA and RNA samples from the green and brown algae collected at all four different sites and all time points (Fig. 7, Table S3). The relative percentage of *Gallionellaceae* was highest in RNA and DNA extracts of the green algae with 89.4-96.5% and 79.5-96.4%, respectively, of the total number of sequence reads compared to 70.4-82.9% and 62.7-81.0% in RNA and DNA extracts of the brown algae. Algal samples collected from sites O, A, B, and C during September showed the lowest fraction of *Gallionellaceae*. The *Gallionellaceae* group comprised of 2 OTUs related to the FeOB *Gallionella capsiferriformans* ES-2 (CP002159) and *Sideroxydans lithotrophicus* ES-1 (CP001965) (Table S3). The relative fraction of OTU-1-related FeOB was highest at site O, whereas OTU-2-related FeOB was more abundant downstream at sites A, B, and C. The dendrograms for each DNA and RNA community also showed that the bacterial community structures in site O were separated from those in other sites (Fig. 7). Other bacterial groups detected with less than 10% relative abundance were '*Candidatus* Odyssella' (*Alphaproteobacteria*), *Actinomycetales* (*Actinobacteria*), *Desulfobulbaceae*, and *Geobacteraceae* (*Deltaproteobacteria*). Triplicate extractions of DNA and RNA from the brown algae collected at site C in August showed little variation between bacterial community structures (Fig. 7), which allows for the identification of a representative algae surface-associated microbial community in this metal-contaminated site. The brown algae were colonized by a

higher diversity of bacterial groups than the green algae, showing higher average Gini-Simpson index values (0.862 in RNA and 0.884 in DNA) than those of the green algae (0.641 in RNA and 0.645 in DNA). Interestingly, some of the sequences detected from the microorganisms adhered to the brown algae surface were identified as putative predators of algae, such as '*Candidatus* Odyssella' (intracellular parasite of Acanthamoeba, up to 8.1% and 6.0% of OTUs in RNA and DNA extracts) and *Cystobacteraceae* (*Myxobacteria*, 2.0% and 0.2% in RNA and DNA extracts).

4. Discussion

Members of the genus *Tribonema* are known as common freshwater algae (Machova et al., 2008; H. Wang et al., 2014). *Tribonema* species have been detected in other metal-rich and acidic freshwater environments such as acidic brown water streams (pH <4) in New Zealand (Collier and Winterbourn, 1990), acidic coal mine drainage-contaminated sites (pH 2.6-6.0) (Winterbourn et al., 2000), as well as acidic rivers (pH 2.7-4.0) with iron-rich ochreous deposits of schwertmannite-like Fe-minerals on algal surfaces (Courtin-Nomade et al., 2005), suggesting their tolerance to high concentrations of metals and low pH. In this study, *T. viride* colonized metal-rich (Fe, Mn, Ni, Zn and U) and less acidic (pH 5.9 to 6.5) mine-water outflow which showed variation in geochemistry over time and along the flow paths from site O to C. The algae ostensibly changed its color from green to brown and disappeared completely from sites B and C at the end of the summer. The change in algae color occurred simultaneously with the loss of active chloroplasts per cell, as observed via CLSM imaging. These results correspond with lower numbers of sequences originating from chloroplasts based on sequences analysis. The encrustation with Fe-minerals presumably inhibits algal photosynthetic activities and may be an underlying cause for the disappearance of *Tribonema* at the end of the summer when light

Deleted: s

Deleted: with pH 5.9 to 6.5

intensity diminished. The observed water temperatures (14-17°C) may have also contributed to the decline in algae numbers, since optimal growth temperatures of two genera of *Tribonema* are higher (*T. fonticolum*, 19-27°C; *T. monochloron*, 15.5-23.5°C) (Machova et al., 2008), however, *T. viride* has been detected in lake water with low temperature (0-5.6°C) (Vinocur and Izaguirre, 1994).

Deposition of Fe-minerals and colonization of "iron bacteria" on *Tribonema* was reported more than 70 years ago (Chapman, 1941), but identification of the deposited minerals, the FeOB, and their interaction with the alga has not been characterized in detail. A symbiotic relationship has been suggested in which microbes living on the surface of *Tribonema* form ferric carbonate, which controls water pH and acts as local buffer for the algae. We could not detect ferric carbonates on *Tribonema*, however, poorly crystalline iron minerals ferrihydrite and schwertmannite that are also present in the underlying sediments in addition to goethite were detected (Johnson et al., 2014). These iron minerals have a high reactive surface area for metal(loid) uptake, and particularly As and Zn appear to be associated with these minerals in the sediments (Johnson et al., 2014). Brown algae showed similar metal(loid) uptake to the sediments collected at the outflow downstream to site C with even higher concentrations for Fe and U suggesting a high affinity of *Tribonema* for these compounds. Thus, these iron coatings could also act as buffers to help prevent the plant from taking up these heavy metals, similar the mechanism suggested to aid in protection from root plaque (Tripathi et al., 2014 and references therein).

Our microscopic investigation did not reveal a preferential colonization of microbes on the algal surface but on the minerals. According to both pyrosequencing and qPCR results, microaerophilic *Gallionella*-related FeOB were the dominant colonizers on *Tribonema* which

Deleted: obtain their oxygen for Fe(II)-oxidation from algal photosynthesis and

Deleted: in turn

might be due to the presence of large populations of *Gallionella* sp. (29-58% of the total bacterial community) in the outflow water reaching cell numbers of 10^5 to 10^6 cells per mL water (Fabisch et al., 2015). These bacteria seem to be able to cope with the high levels of oxygen produced during photosynthesis, but these oxygen concentrations may be lower within the EPS matrix and ochre deposits. *G.capsiferriformans*-related FeOB predominated at the outflow site whereas *S. lithotrophicus*-related FeOB dominated algae further downstream which can be explained by differences in the water geochemistry such as pH or heavy metal concentrations. Based on genome information, *G. capsiferriformans* ES-2 should be more resistant to heavy metals than *S. lithotrophicus* ES-1 (Emerson et al., 2013) and thus should dominate the outflow site which showed the highest metal loads in the water. Unfortunately, we could not link the dominance of these species with the heavy metals precipitated on the algae due to shortage of the present sample amount for ICP-MS/OES.

16S rRNA gene copy numbers of *Gallionella* on the algae surfaces (Table 1) were much higher than numbers found in the sediments of the stream (3.1 x 10^8 copies per gram wet weight sediment) (Fabisch et al., 2015). The high relative RNA-derived fraction of *Gallionellaceae* suggested not only passive or active colonization of the algal surface but also participation in Fe-oxidation followed by ferrihydrite and schwertmannite formation. *Gallionella*-related FeOB appeared to be more abundant and active on the green algae, which indicates higher Fe-oxidizing activity on the surface of green algae. The surface of photosynthetic algae is presumable a highly oxygen-saturated environment, and the occurrence of neutrophilic microaerophilic FeOB under such conditions has not been reported before to the best of our knowledge. However, it is possible that at night the oxygen level go to a much lower level allowing an opportunity for FeOB to grow under low oxygen. In water treatment systems and dewatering wells in open cast

Deleted: *S. lithotrophicus*

Deleted: *G. capsiferriformans*

Deleted: ¶

mines, *Gallionella* have been also reported to grow at surprisingly high oxygen concentrations at the low temperature of 13˚C or even higher which slows down abiotic Fe(II)-oxidation (de Vet et al., 2011; J. Wang et al., 2014).

In an Fe(II)-rich and oxygenated environment, bacteria potentially face the problem of highly reactive oxygen species due to the reaction of hydrogen peroxide with Fe(II) (Imlay, 2008). Both *G. capsiferriformans* ES-2 and *S. lithotrophicus* ES-1 were reported to encode enzymes that presumably act as catalase or peroxidase to prevent production of reactive oxygen species (Emerson et al., 2013). Most bacteria associated with the Fe-minerals on algae surfaces were also localized to areas where EPS-like glycoconjugates were detected. EPS forms a suitable microenvironment for microbial Fe-oxidation due to its ability to bind dissolved Fe(II) resulting from the negatively charged EPS matrix. This activity leads to the inhibition of chemical Fe-oxidation by lowering the availability of Fe(II) (Neubauer et al., 2002; Jiao et al., 2010; Roth et al., 2000). In addition, the EPS can prevent bacterial cells from being encrusted with insoluble Fe(III)-oxides (Neubauer et al., 2002; Hedrich et al., 2011a; Schädler et al., 2009). Unfortunately, with the methods used, we could not determine if the EPS-like matrix on the algae was produced by the alga or by bacteria. *Tribonema* is known to produce EPS mainly composed of glucans and xylans (Cleare and Percival, 1972), however, based on genome sequencing both *G. capsiferriformas* ES-2 and *S. lithotrophicus* ES-1 are predicted to also produce EPS (Emerson et al., 2013). In an effort to prevent encrustation, other *Gallionella* species form long stalks which are mainly composed of polysaccharides and long-chain saturated aliphatic compounds during Fe(II)-oxidation with the purpose of deposition of Fe-oxides apart from the cells (Chan et al., 2011; Suzuki et al., 2011; Fabisch et al., 2015; Picard et al., 2015). Stalk-forming *Gallionella* have been isolated in sediment environments, but not on the surface of algae, thus implicating an

Deleted: the

Deleted: The

Deleted: composed of polysaccharides where Fe-oxides are deposited

Deleted: Hanert, 1981

Deleted: which implies EPS plays an important role for

important role of EPS in microbial Fe-oxidation by the algae-associated bacteria. Since *G. capsiferriformans* and *S. lithotrophicus* were reported to be unable to grow heterotrophically (Emerson et al., 2013), algal EPS is not suspected to be used as organic carbon source by the FeOB. The variations in color of the *Tribonema* species were accompanied with a variation in encrustation patterns. The green *Tribonema* was fully encrusted whereas the brown *Tribonema* showed an irregular encrustation pattern. Although *Tribonema* appears to be adapted to high metal loads, excess encrustations with Fe-minerals should be detrimental due to inhibition of photosynthesis and decreased access to nutrients. The lower number of chloroplast pointed to decreased photosynthetic activity of the brown *Tribonema*. The discontinuous encrustation might be caused by intercalary growth of the filamentous algae, which occurs by generating H-shaped parts in the middle of each cell (Smith, 1938). Intercalary growth was confirmed by CLSM images with lectin staining which showed algal cell sections alternating with Fe-minerals. The new cell sections were thin with only a few chloroplasts suggesting that energy was used primarily for elongation. Thus, intercalary growth could be interpreted as a defense strategy during later stages of encrustation when photosynthetic activity diminishes due to surface coverage by Fe-precipitates and to provide the algae with new uncovered cell surfaces.

Production of EPS as a shunt mechanism should decline if less carbon is fixed during photosynthesis (Wotton, 2004) which provides a potential link between EPS production and *Gallionella* colonization. Brown algae contained fewer chloroplasts, suggesting reduced photosynthetic activity and EPS production which might be linked to a decrease in *Gallionella* cell number and Fe(II) oxidation on the algae surface. This study showed higher microbial diversity on the surface of brown *Tribonema* when lower numbers of *Gallionella* were detected. Some putative predators of algae, such as '*Candidatus* Odyssella' and *Cystobacteraceae* were

Deleted: fatal

Deleted: indicating

Deleted: leading

also identified on the surface of the brown *Tribonema*. These predators colonize algae in order to consume material released upon cell lysis as a natural senescence process or under stress conditions (Levy et al., 2009). Algal EPS has been shown to function as a cell defense mechanism to protect cells from colonization of predators or pathogens (Steinberg et al., 1997), thus a reduced rate of EPS formation may lead to predator colonization.

5. Summary and Conclusion

Filamentous algae (*Tribonema* sp.) were observed in the metal-contaminated groundwater outflow in the former Ronneburg uranium mining district, suggesting the algae has a tolerance to high metal concentrations and metal deposits. Cells of green algae were fully encrusted with Fe-oxides. The Fe-precipitates on the algae surfaces were predominantly colonized by *Gallionella*-related FeOB. *Gallionella*-related FeOB were abundant in the stream water and these bacteria appeared to be actively involved in Fe(II) oxidation. Thus, both sunlight and Fe(II) served as energy sources for primary producers in this slightly acidic stream promoting complex microbial interactions in the ochre deposits on the algal cells. EPS-like polymeric matrices, likely produced as a shunt for carbon during photosynthesis, provided a suitable microenvironment for the microaerophilic FeOB due to its high affinity for metal(loid)s and reduced oxygen diffusion. However, excess deposition of Fe-oxides appeared to be detrimental to photosynthetic activities forcing intercalary elongation of the filaments. This defense response caused discontinuous deposition patterns of Fe-oxides as observed on the brown colored algae which showed lower number of chloroplasts. The reduced EPS production could have favored growth of algal predators on the brown algae and together with ochre deposition contributed to algal decline.

Deleted: The f
Deleted: yellow-green
Deleted: fatal
Deleted: for

Author contribution

J. F. Mori and K. Küsel designed and J. F. Mori performed the experiments. T. R. Neu conducted CLSM imaging analysis. S. Lu carried out sampling and microscopic analysis with J. F. Mori. M. Händel and K. U. Totsche performed SEM-EDX and FTIR analysis. J. F. Mori prepared the manuscript with contributions from all co-authors.

Acknowledgements

The authors thank the graduate research training group "Alternation and element mobility at the microbe-mineral interface" (GRK 1257), which is part of the Jena School for Microbial Communication (JSMC) and funded by the Deutsche Forschungsgemeinschaft (DFG) for financial support. We would also like to thank Denise M. Akob and Georg Büchel for help during sampling. We appreciate Martina Herrmann for sequence analysis, Maren Sickinger for qPCR works, Dirk Merten for ICP measurements, Gundula Rudolph for DOC analysis, Steffen Kolb, Juanjuan Wang, and Maria Fabisch for helpful discussions and Rebecca Cooper for manuscript proofreading.

Reference

Akiyama, M., Ioriya, T., Imahori, K., Kasaki, H., Kumamoto, S., Kobayashi, H., Takahashi, E., Tsumura, K., Hirano, M., and Hirose, H.: Illustrations of the Japanese Fresh-Water Algae, Uchidarokakuho Publishing Company, Limited, 1977.

Azam, F.: Microbial control of oceanic carbon flux: the plot thickens, Science, 280, 694-695, 1998.

Bray, J. R., and Curtis, J. T.: An ordination of the upland forest communities of southern Wisconsin, Ecol. Monogr., 27, 325-349, 1957.

Cantonati, M., and Lowe, R. L.: Lake benthic algae: toward an understanding of their ecology, Freshwater, 33, 475-486, 2014.

Carlson, L., Bigham, J. M., Schwertmann, U., Kyek, A., and Wagner, F.: Scavenging of As from acid mine drainage by schwertmannite and ferrihydrite: a comparison with synthetic analogues, Environ. Sci. Technol., 36, 1712-1719, doi:10.1021/es0110271, 2002.

Chan, C. S., Fakra, S. C., Emerson, D., Fleming, E. J., and Edwards, K. J.: Lithotrophic iron-oxidizing bacteria produce organic stalks to control mineral growth: implications for biosignature formation, ISME J., 5, 717-727, doi:10.1038/ismej.2010.173, 2011.

Chapman, V. J.: An introduction to the study of Algae, Cambrige University Press, 387, 1941.

Cleare, M., and Percival, E.: Carbohydrates of the fresh water alga *Tribonema aequale*. I. Low molecular weight and polysaccharides, Brit. Phycol. J., 7, 185-193, doi:10.1080/00071617200650201, 1972.

Cole, J. J.: Interactions between bacteria and algae in aquatic ecosystems, Annu. Rev. Ecol. Syst., 13, 291-314, 1982.

Deleted: Bond, P. L., Smriga, S. P., and Banfield, J. F.: Phylogeny of microorganisms populating a thick, subaerial, predominantly lithotrophic biofilm at an extreme acid mine drainage site, Appl. Environ. Microb., 66, 3842-3849, doi:10.1128/aem.66.9.3842-3849.2000, 2000.¶

Deleted: Chan, C. S., De Stasio, G., Welch, S. A., Girasole, M., Frazer, B. H., Nesterova, M. V., Fakra, S., and Banfield, J. F.: Microbial polysaccharides template assembly of nanocrystal fibers, Science, 303, 1656-1658, doi:10.1126/science.1092098, 2004.¶

Collier, K., and Winterbourn, M.: Structure of epilithon in some acidic and circumneutral streams in South Westland, New Zealand, New Zealand Natural Sciences, 17, 1-11, 1990.

Colmer, A. R., and Hinkle, M.: The role of microorganisms in acid mine drainage: a preliminary report, Science, 106, 253-256, 1947.

Courtin-Nomade, A., Grosbois, C., Bril, H., and Roussel, C.: Spatial variability of arsenic in some iron-rich deposits generated by acid mine drainage, Appl. Geochem., 20, 383-396, doi:10.1016/j.apgeochem.2004.08.002, 2005.

Das, B. K., Roy, A., Koschorreck, M., Mandal, S. M., Wendt-Potthoff, K., and Bhattacharya, J.: Occurrence and role of algae and fungi in acid mine drainage environment with special reference to metals and sulfate immobilization, Water Res., 43, 883-894, doi:10.1016/j.watres.2008.11.046, 2009.

de Vet, W. W. J. M., Dinkla, I. J. T., Rietveld, L. C., and van Loosdrecht, M. C. M.: Biological iron oxidation by *Gallionella* spp. in drinking water production under fully aerated conditions, Water Res., 45:17, 5389-5398, doi:10.1016/j.watres.2011.07.028, 2011.

Dorigo, U., Berard, A., and Humbert, J. F.: Comparison of eukaryotic phytobenthic community composition in a polluted river by partial 18S rRNA gene cloning and sequencing, Microb. Ecol., 44, 372-380, doi:10.1007/s00248-002-2024-x, 2002.

Emerson, D., and Moyer, C.: Isolation and characterization of novel iron-oxidizing bacteria that grow at circumneutral pH, Appl. Environ. Microb., 63, 4784-4792, 1997.

Emerson, D., and Weiss, J. V.: Bacterial iron oxidation in circumneutral freshwater habitats: findings from the field and the laboratory, Geomicrobiol. J., 21, 405-414, 2004.

601 Emerson, D., Weiss, J. V., and Megonigal, J. P.: Iron-oxidizing bacteria are associated with
602 ferric hydroxide precipitates (Fe-plaque) on the roots of wetland plants, Appl. Environ.
603 Microb., 65, 2758-2761, 1999.
604 Emerson, D., Field, E., Chertkov, O., Davenport, K., Goodwin, L., Munk, C., Nolan, M., and
605 Woyke, T.: Comparative genomics of freshwater Fe-oxidizing bacteria: implications for
606 physiology, ecology, and systematics, Front. Microbiol., 4:254,
607 doi:10.3389/fmicb.2013.00254, 2013.
608 Euringer, K., and Lueders, T.: An optimised PCR/T-RFLP fingerprinting approach for the
609 investigation of protistan communities in groundwater environments, J. Microbiol. Meth., 75,
610 262-268, doi:10.1016/j.mimet.2008.06.012, 2008.
611 Fabisch, M., Beulig, F., Akob, D. M., and Küsel, K.: Surprising abundance of *Gallionella*-related
612 iron oxidizers in creek sediments at pH 4.4 or at high heavy metal concentrations, Front.
613 Microbiol., 4:390, doi:10.3389/fmicb.2013.00390, 2013.
614 Fabisch, M., Freyer, G., Johnson, C. A., Büchel, G., Akob, D. M., Neu, T. R., and Küsel, K.:
615 Dominance of '*Gallionella capsiferriformans*' and heavy metal association with *Gallionella*-
616 like stalks in metal-rich pH 6 mine water discharge, Geobiology, submitted, 2015.
617 Fisher, M., Zamir, A., and Pick, U.: Iron uptake by the halotolerant alga *Dunaliella* is mediated
618 by a plasma membrane transferrin, J. Biol. Chem., 273, 17553-17558, 1998.
619 Foster, P. L.: Copper exclusion as a mechanism of heavy metal tolerance in a green alga, Nature,
620 269, 322-323, 1977.
621 Foster, P. L.: Metal resistances of *Chlorophyta* from rivers polluted by heavy metals, Freshwater
622 Biol., 12, 41-61, 1982.

623 Gebühr, C., Pohlon, E., Schmidt, A., and Küsel, K.: Development of microalgae communities in
624 the phytotelmata of allochthonous populations of *Sarracenia purpurea* (Sarraceniaceae),
625 Plant Biol., 8, 849-860, 2006.
626 Geesey, G., Mutch, R., Costerton, J. t., and Green, R.: Sessile bacteria: an important component
627 of the microbial population in small mountain streams, Limnol. Oceanogr., 23, 1214-1223,
628 1978.
629 Greene, B., McPherson, R., and Darnall, D.: Algal sorbents for selective metal ion recovery, in:
630 Metals Speciation, Separation, and Recovery, Lewis Publishers Chelsea, MI, 315-338, 1987.
631 Gudleifsson, B. E.: *Tribonema viride* (*Xanthophyta*) on cultivated grassland during winter and
632 spring, Acta Botanica Islandica, 7, 27-30, 1984.
633 Haack, T. K., and McFeters, G. A.: Microbial dynamics of an epilithic mat community in a high
634 alpine stream, Appl. Environ. Microb., 43, 702-707, 1982.
635 Hallberg, K. B., Coupland, K., Kimura, S., and Johnson, D. B.: Macroscopic streamer growths in
636 acidic, metal-rich mine waters in north wales consist of novel and remarkably simple
637 bacterial communities, Appl. Environ. Microb., 72, 2022-2030, doi:10.1128/aem.72.3.2022-
638 2030.2006, 2006.
639 Hanert, H. H.: The genus *Gallionella*, in: The prokaryotes, Springer Verlag, New York, 990-995,
640 2006.
641 Hedrich, S., Lunsdorf, H., Keeberg, R., Heide, G., Seifert, J., and Schlomann, M.:
642 Schwertmannite formation adjacent to bacterial cells in a mine water treatment plant and in
643 pure cultures of *Ferrovum myxofaciens*, Environ. Sci. Technol., 45, 7685-7692,
644 doi:10.1021/es201564g, 2011a.

645 Hedrich, S., Schlomann, M., and Johnson, D. B.: The iron-oxidizing proteobacteria,
646 Microbiology, 157, 1551-1564, doi:10.1099/mic.0.045344-0, 2011b.
647 Hegler, F., Lösekann-Behrens, T., Hanselmann, K., Behrens, S., and Kappler, A.: Influence of
648 seasonal and geochemical changes on the geomicrobiology of an iron carbonate mineral
649 water spring, Appl. Environ. Microb., 78, 7185-7196, doi:10.1128/aem.01440-12, 2012.
650 Heinzel, E., Janneck, E., Glombitza, F., Schlömann, M., and Seifert, J.: Population dynamics of
651 iron-oxidizing communities in pilot plants for the treatment of acid mine waters, Environ. Sci.
652 Technol., 43, 6138-6144, 2009.
653 Imlay, J. A.: Cellular defenses against superoxide and hydrogen peroxide, Annu. Rev. Biochem.,
654 77, 755-776, doi:10.1146/annurev.biochem.77.061606.161055, 2008.
655 Jiao, Y., Cody, G. D., Harding, A. K., Wilmes, P., Schrenk, M., Wheeler, K. E., Banfield, J. F.,
656 and Thelen, M. P.: Characterization of extracellular polymeric substances from acidophilic
657 microbial biofilms, Appl. Environ. Microb., 76, 2916-2922, doi:10.1128/aem.02289-09, 2010.
658 Johnson, C. A., Freyer, G., Fabisch, M., Caraballo, M. A., Küsel, K., and Hochella, M. F.:
659 Observations and assessment of iron oxide and green rust nanoparticles in metal-polluted
660 mine drainage within a steep redox gradient, Environ. Chem., 11, 377-391,
661 doi:10.1071/EN13184, 2014.
662 Johnson, D. B., and Hallberg, K. B.: Carbon, iron and sulfur metabolism in acidophilic micro-
663 organisms, Adv. Microb. Physiol., 54, 201-255, doi:10.1016/s0065-2911(08)00003-9, 2009.
664 Johnsongreen, P. C., and Crowder, A. A.: Iron-oxide deposition on axenic and non-axenic roots
665 of rice seedlings (*Oryza sativa* L.), J. Plant Nutr., 14, 375-386,
666 doi:10.1080/01904169109364209, 1991.

Deleted: a

Deleted: Johnson, D. B., Hallberg, K. B., and Hedrich, S.: Uncovering a microbial enigma: isolation and characterization of the streamer-generating, iron-oxidizing, acidophilic bacterium "*Ferrovum myxofaciens*", Appl. Environ. Microb., 80, 672-680, 2014b.¶

674 Kappler, A., and Straub, K. L.: Geomicrobiological cycling of iron, Rev. Mineral. Geochem., 59,
675 85-108, 2005.
676 Kozubal, M. A., Macur, R. E., Jay, Z. J., Beam, J. P., Malfatti, S. A., Tringe, S. G., Kocar, B. D.,
677 Borch, T., and Inskeep, W. P.: Microbial iron cycling in acidic geothermal springs of
678 Yellowstone National Park: integrating molecular surveys, geochemical processes, and
679 isolation of novel Fe-active microorganisms, Front. Microbiol., 3:109,
680 doi:10.3389/fmicb.2012.00109, 2012.
681 Leduc, L. G., and Ferroni, G. D.: The chemolithotrophic bacterium *Thibacillus ferrooxidans*,
682 FEMS Microbiol. Rev., 14, 103-119, 1994.
683 Levy, J., Stauber, J. L., Wakelin, S. A., and Jolley, D. F.: The effect of bacteria on the sensitivity
684 of microalgae to copper in laboratory bioassays, Chemosphere, 74, 1266-1274,
685 doi:10.1016/j.chemosphere.2008.10.049, 2009.
686 Liu, H., and Buskey, E. J.: Hypersalinity enhances the production of extracellular polymeric
687 substance (EPS) in the Texas brown tide alga, *Aureoumbra lagunensis* (Pelagophyceae), J.
688 Phycol., 36, 71-77, 2000.
689 López-Archilla, A. I., Marin, I., and Amils, R.: Microbial community composition and ecology
690 of an acidic aquatic environment: the Tinto River, Spain, Microb. Ecol., 41, 20-35, 2001.
691 Lüdecke, C., Reiche, M., Eusterhues, K., Nietzsche, S., and Küsel, K.: Acid-tolerant
692 microaerophilic Fe(II)-oxidizing bacteria promote Fe(III)-accumulation in a fen, Environ.
693 Microbiol., 12, 2814-2825, doi:10.1111/j.1462-2920.2010.02251.x, 2010.
694 Machova, K., Elster, J., and Adamec, L.: Xanthophyceaen assemblages during winter-spring
695 flood: autecology and ecophysiology of *Tribonema fonticolum* and *T. monochloron*,
696 Hydrobiologia, 600, 155-168, doi:10.1007/s10750-007-9228-5, 2008.

Deleted: Kay, C. M., Rowe, O., Rocchetti, L., Coupland, K., Hallberg, K., and Johnson, D.: Evolution of microbial "streamer" growths in an acidic, metal-contaminated stream draining an abandoned underground copper mine, Life (Basel), 3, 189-210, 2013.¶

Malik, A.: Metal bioremediation through growing cells, Environ. Int., 30, 261-278, 2004.

Neu, T. R., Swerhone, G. D., and Lawrence, J. R.: Assessment of lectin-binding analysis for in situ detection of glycoconjugates in biofilm systems, Microbiology, 147, 299-313, 2001.

Neubauer, S. C., Emerson, D., and Megonigal, J. P.: Life at the energetic edge: kinetics of circumneutral iron oxidation by lithotrophic iron-oxidizing bacteria isolated from the wetland-plant rhizosphere, Appl. Environ. Microb., 68, 3988-3995, doi:10.1128/aem.68.8.3988-3995.2002, 2002.

Peine, A., Tritschler, A., Küsel, K., and Peiffer, S.: Electron flow in an iron-rich acidic sediment - evidence for an acidity-driven iron cycle, Limnol. Oceanogr., 45, 1077-1087, 2000.

Picard, A., Kappler, A., Schmid, G., Quaroni, L., and Obst, M.: Experimental diagenesis of organo-mineral structures formed by microaerophilic Fe(II)-oxidizing bacteria, Nature Communications, 6, 6277, doi:10.1038/ncomms7277, 2015.

Reed, R., and Gadd, G.: Metal tolerance in eukaryotic and prokaryotic algae, in: Heavy Metal Tolerance in Plants: Evolutionary Aspects, CRC press, Boca Raton, FL, 105-118, 1989.

Roth, R. I., Panter, S. S., Zegna, A. I., and Levin, J.: Bacterial endotoxin (lipopolysaccharide) stimulates the rate of iron oxidation, J. Endotoxin Res., 6, 313-319, 2000.

Rowe, O. F., Sanchez-Espana, J., Hallberg, K. B., and Johnson, D. B.: Microbial communities and geochemical dynamics in an extremely acidic, metal-rich stream at an abandoned sulfide mine (Huelva, Spain) underpinned by two functional primary production systems, Environ. Microbiol., 9, 1761-1771, doi:10.1111/j.1462-2920.2007.01294.x, 2007.

Schädler, S., Burkhardt, C., Hegler, F., Straub, K. L., Miot, J., Benzerara, K., and Kappler, A.: Formation of cell-iron-mineral aggregates by phototrophic and nitrate-reducing anaerobic

725 Fe(II)-oxidizing bacteria, Geomicrobiol. J., 26:2, 93-103, doi:10.1080/01490450802660573,
726 2009.
727 Schloss, P. D., Westcott, S. L., Ryabin, T., Hall, J. R., Hartmann, M., Hollister, E. B.,
728 Lesniewski, R. A., Oakley, B. B., Parks, D. H., and Robinson, C. J.: Introducing mothur:
729 open-source, platform-independent, community-supported software for describing and
730 comparing microbial communities, Appl. Environ. Microb., 75, 7537-7541, 2009.
731 Sengbusch, P. V., and Müller, U.: Distribution of glycoconjugates at algal cell surfaces as
732 monitored by FITC-conjugated lectins. Studies on selected species from *Cyanophyta*,
733 *Pyrrhophyta*, *Raphidophyta*, *Euglenophyta*, *Chromophyta*, and *Chlorophyta*, Protoplasma,
734 114, 103-113, 1983.
735 Senko, J. M., Wanjugi, P., Lucas, M., Bruns, M. A., and Burgos, W. D.: Characterization of
736 Fe(II) oxidizing bacterial activities and communities at two acidic Appalachian coalmine
737 drainage-impacted sites, ISME J., 2, 1134-1145, 2008.
738 Smith, G. M.: Cryptogamic Botany, Vol. 1, Algae and Fungi, McGraw-Hill, New York, 1938.
739 Steinberg, P. D., Schneider, R., and Kjelleberg, S.: Chemical defenses of seaweeds against
740 microbial colonization, Biodegradation, 8, 211-220, doi:10.1023/a:1008236901790, 1997.
741 Stevenson, R. J., Bothwell, M. L., Lowe, R. L., and Thorp, J. H.: Algal ecology: Freshwater
742 Benthic Ecosystem, Academic press, San Diego, 1996.
743 Suzuki, T., Hashimoto, H., Matsumoto, N., Furutani, M., Kunoh, H., and Takada, J.: Nanometer-
744 scale visualization and strucural analysis of the inorganic/organic hybrid structures of
745 *Gallionella ferruginea* twisted stalks, Appl. Environ. Microb., 77, 2877-2881,
746 doi:10.1128/aem.02867-10, 2011.

747 Tabatabai, M. A.: A rapid method for determination of sulfate in water samples, Environ. Lett., 7,
748 237-243, 1974.
749 Tamura, H., Goto, K., Yotsuyan.T, and Nagayama, M.: Spectrophotometric determination of
750 iron(II) with 1,10-phenanthroline in presence of large amounts of iron(III), Talanta, 21, 314-
751 318, doi:10.1016/0039-9140(74)80012-3, 1974.
752 Tang, Y. Z., and Dobbs, F. C.: Green autofluorescence in dinoflagellates, diatoms, and other
753 microalgae and its implications for vital staining and morphological studies, Appl. Environ.
754 Microb., 73, 2306-2313, doi:10.1128/aem.01741-06, 2007.
755 Transeau, E. N.: The periodicity of freshwater algae, Am. J. Bot., 3, 121-133, 1916.
756 Tripathi, R. D., Tripathi, P., Dwivedi, S., Kumar, A., Mishra, A., Chauhan, P. S., Norton, G. J.,
757 and Nautiyal, C. S.: Roles for root iron plaque in sequestration and uptake of heavy metals
758 and metalloids in aquatic and wetland plants, Metallomics, 6, 1789-1800,
759 doi:10.1039/c4mt00111g, 2014.
760 Trouwborst, R. E., Johnston, A., Koch, G., Luther, G. W., and Pierson, B. K.: Biogeochemistry
761 of Fe(II) oxidation in a photosynthetic microbial mat: implications for Precambrian Fe(II)
762 oxidation, Geochim. Cosmochim. Acta, 71:19, 4629-4643, doi:10.1016/j.gca.2007.07.018,
763 2007.
764 Tyson, G. W., Chapman, J., Hugenholtz, P., Allen, E. E., Ram, R. J., Richardson, P. M.,
765 Solovyev, V. V., Rubin, E. M., Rokhsar, D. S., and Banfield, J. F.: Community structure and
766 metabolism through reconstruction of microbial genomes from the environment, Nature, 428,
767 37-43, doi:10.1038/nature02340, 2004.
768 Vinocur, A., and Izaguirre, I.: Freshwater algae (excluding *Cyanophyceae*) from nine lakes and
769 pools of Hope Bay, Antarctic Peninsula, Antarct. Sci., 6, 483-490, 1994.

Wang, H., Ji, B., Wang, J., Guo, F., Zhou, W., Gao, L., and Liu, T.: Growth and biochemical composition of filamentous microalgae *Tribonema* sp. as potential biofuel feedstock, Bioproc. Biosyst. Eng., 37, 2607-2613, 2014.

Wang, J., Sickinger, M., Ciobota, V., Herrmann, M., Rasch, Helfried, Rösch, P., Popp, J., and Küsel, K.: Revealing the microbial community structure of clogging materials in dewatering wells differing in physico-chemical parameters in an open-cast mining area, Water Res., 63:15, 222-233, doi:10.1016/j.watres.2014.06.021, 2014.

Warner, R. W.: Distribution of biota in a stream polluted by acid mine-drainage, Ohio J. Sci., 71, 202-215, 1971.

Wiegert, R. G., and Mitchell, R.: Ecology of Yellowstone thermal effluent systems: intersects of blue-green algae, grazing flies (*Paracoenia*, Ephydridae) and water mites (*Partnuniella*, Hydrachnellae), Hydrobiologia, 41, 251-271, 1973.

Winterbourn, M. J., McDiffett, W. F., and Eppley, S. J.: Aluminium and iron burdens of aquatic biota in New Zealand streams contaminated by acid mine drainage: effects of trophic level, Sci. Total Environ., 254, 45-54, doi:10.1016/s0048-9697(00)00437-x, 2000.

Wotton, R. S.: The utiquity and many roles of exopolymers (EPS) in aquatic systems, Sci. Mar., 68, 13-21, 2004.

Yu, Q., Matheickal, J. T., Yin, P., and Kaewsarn, P.: Heavy metal uptake capacities of common marine macro algal biomass, Water Res., 33, 1534-1537, 1999.

Deleted: Wakao, N., Tachibana, H., Tanaka, Y., Sakurai, Y., and Shiota, H.: Morphological and physiological-characterstics of streamers in acid-mine drainage water from a pyritic mine, J. Gen. Appl. Microbiol., 31, 17-28, doi:10.2323/jgam.31.17, 1985.¶

Tables & Figures

Table 1. Average 16S rRNA gene copy numbers of *Gallionella* detected per gram wet weight algae sampled at sites O, A, B, and C, and at three sampling times in 2013 and measured by quantitative PCR (n=3, ± SD).

	Site O	Site A	Site B	Site C
July 2013	Not reachable	Green $1.85 \times 10^9 \pm 1.86 \times 10^7$	Green $1.72 \times 10^9 \pm 1.62 \times 10^8$	Brown $0.95 \times 10^9 \pm 6.66 \times 10^7$
August 2013	Green $6.78 \times 10^9 \pm 2.36 \times 10^8$	Green $7.08 \times 10^9 \pm 3.76 \times 10^8$	Brown $1.45 \times 10^9 \pm 1.07 \times 10^8$	Brown $1.25 \times 10^9 \pm 1.62 \times 10^7$
September 2013	Green $2.25 \times 10^9 \pm 1.19 \times 10^7$	Brown $1.10 \times 10^9 \pm 3.47 \times 10^7$	No algae	No algae

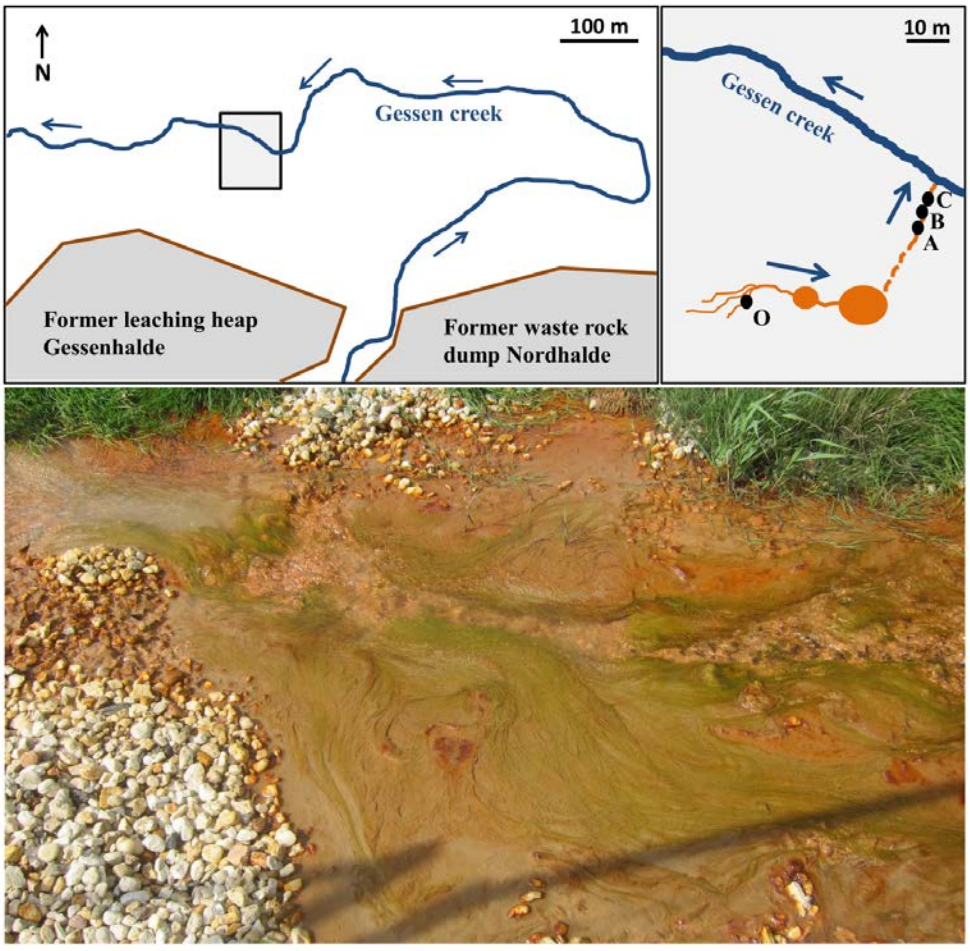

802

803 **Figure 1.** Schematic maps of the study site and photograph of the site A in the former
804 Ronneburg uranium mining district (Thuringia, Germany). Maps show the locations of sampling
805 sites O, A, B and C on the grassland close to Gessen creek. Blue arrows indicate the flow
806 direction of the creek and outflow streams. The photograph was taken in September 2011 and
807 shows the presence of conspicuous green filamentous algae.

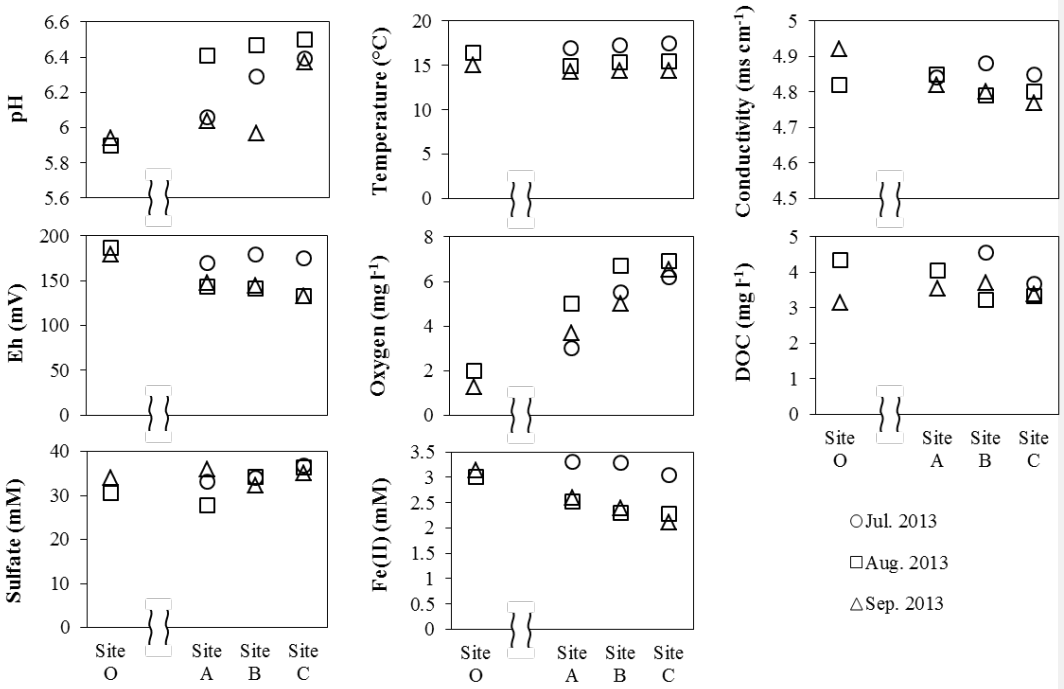

808

809 **Figure 2.** Chemical parameters of water at each sampling site in the outflow water stream. Water
810 pH, oxygen, temperature, conductivity and Eh were measured in the field at site O, A, B and C in
811 July, August, and September 2013. Concentrations of organic carbon, sulfate and Fe(II) were
812 determined later in the laboratory.

813

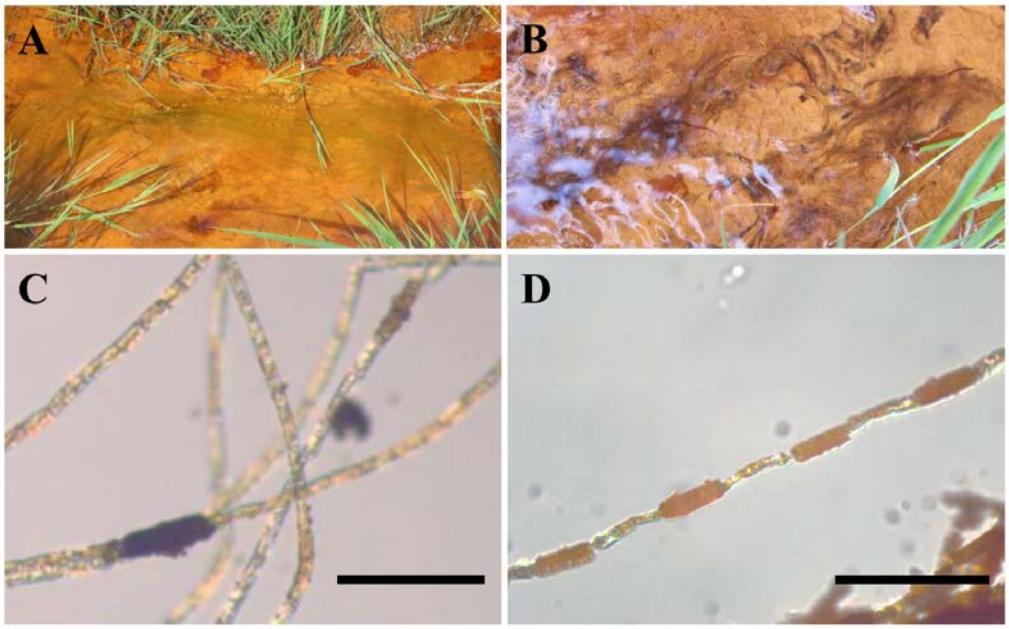

814

815 **Figure 3.** Photographs (A, B) and light microscopic pictures (C, D) of the green algae in site A
816 (A, C) and the brown algae in site C (B, D) taken in July 2013. The microscopic pictures show
817 Fe-mineral precipitates on the algae. Scale bars indicate 100 µm.

818

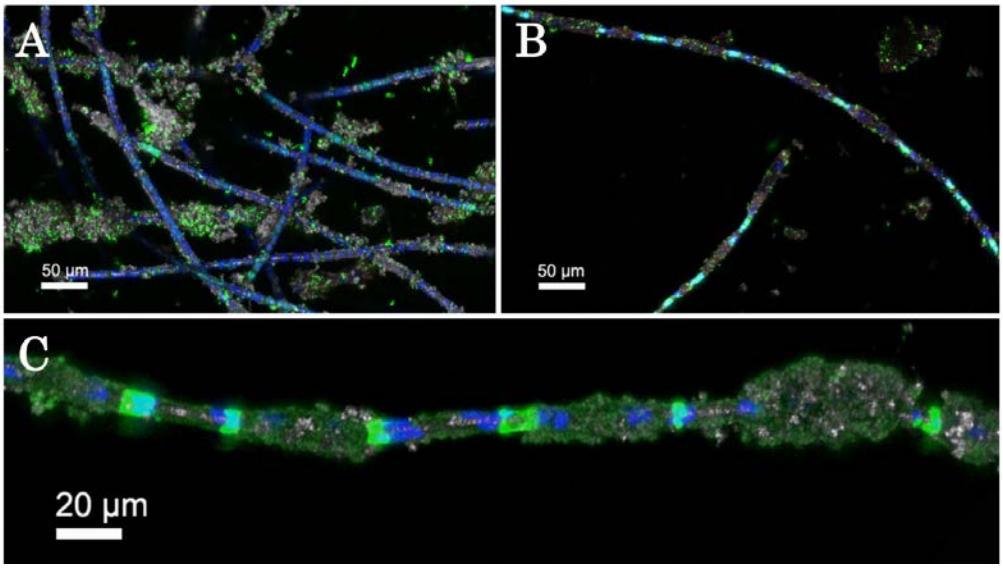

819

820 **Figure 4.** Confocal laser scanning microscopy images of the algae-microbial communities
821 collected at site O (outflow) of the stream in September 2013. Maximum intensity projection of
822 the green algae (A) and the brown algae (B) stained with Syto9 were recorded (color allocation:
823 green – nucleic acid stain; blue – autofluorescence of chlorophyll A; grey - reflection). Brown
824 algae stained with AAL-Alexa448 (C) shows glycoconjugates (green), autofluorescence of
825 chlorophyll A (blue), and refection (grey).

826

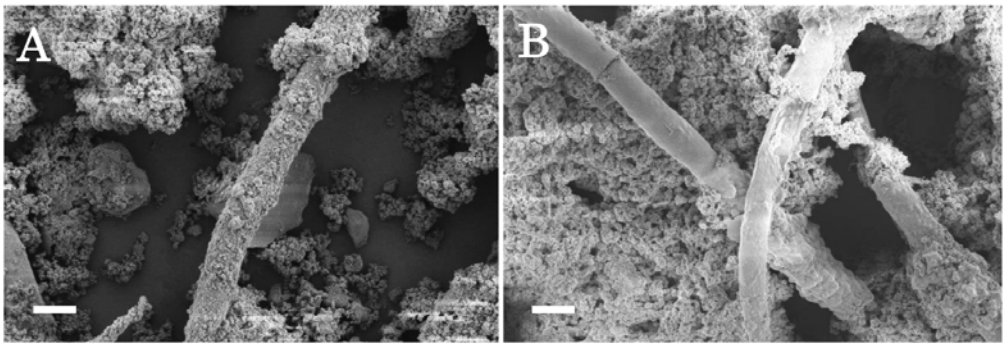

827

828 **Figure 5.** Scanning electron microscopy images of the green algae in site O (A) and the brown
829 algae in site A (B) taken in September 2013. Scale bars indicate 10 µm.

830

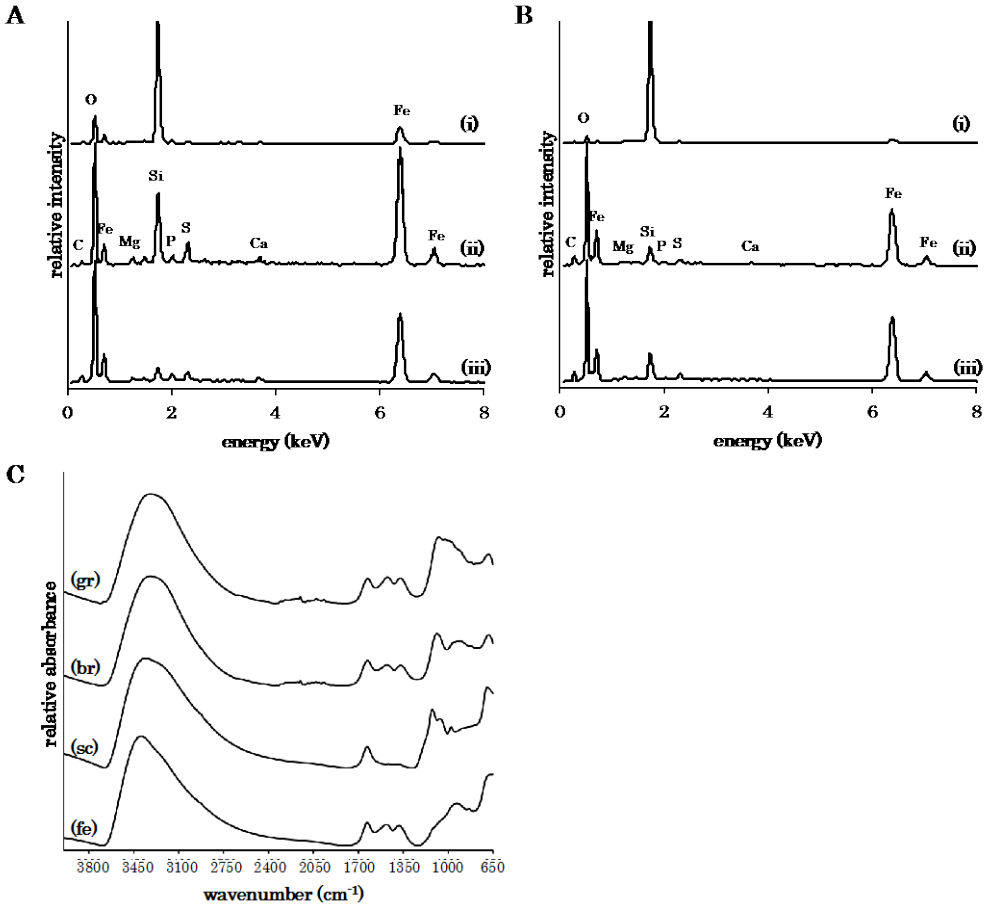

831

832 **Figure 6.** EDX and FTIR spectra of minerals precipitated around the algae. EDX spectra of
833 minerals around the green algae (a) and the brown algae (b) were recorded on the non-encrusted
834 algal surface (i), the encrusted algal surface (ii) and Fe-oxides which were not connected to the
835 algae (iii). FTIR spectra of Fe-oxides (c) were recorded on the green algae (gr) and the brown
836 algae (br), comparing with spectra of schwertmannite (sc) and ferrihydrite (fe) as references.

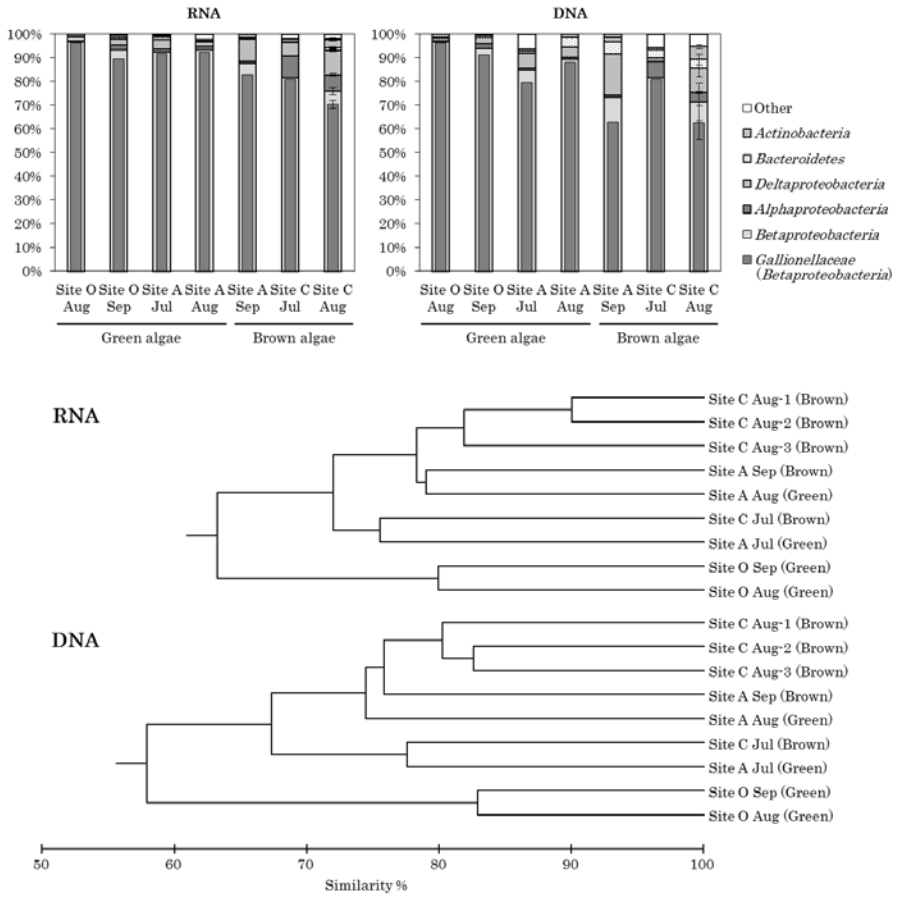

Figure 7. Bacterial community compositions obtained from algal samples detected by 16S rRNA gene-targeted amplicon pyrosequencing (above) and dendrograms indicating similarities of RNA and DNA compositions (below). Calculations of the bacterial populations were based on the total numbers of OTUs associated with phylotypes of sequenced representatives at the phylum level, or class level for Proteobacteria. Percentages of *Gallionellaceae* (*Betaproteobacteria*) were also shown. (n=1; Site C Aug, n=3, error bars indicate SD)